RECENT SIMULATION CONCLUSIONS FOR DAMPED-OSCILLATION CONTROL OF CRANES

R. L. Kress
Dept. of Mechanical and Aerospace Engineering and Engineering Science
The University of Tennessee
Knoxville, Tennessee 37996-2210
Phone: 865-974-5275 email: rkress@utk.edu

M. W. Noakes
Oak Ridge National Laboratory
Robotics & Process Systems Division
P.O. Box 2008, Building 7601
Oak Ridge, Tennessee 37831-6426
Phone: 865-974-5695 email: noakesmw@ornl.gov

ABSTRACT

When suspended payloads are moved with an overhead crane, pendulum like oscillations are naturally introduced. This presents a problem any time a crane is used, especially when expensive and/or delicate objects are moved, when moving in a cluttered and/or hazardous environment, and when objects are to be placed in tight locations. For example, one nuclear waste-handling operation examined by the U.S. Department of Energy (DOE) Oak Ridge National Laboratory (ORNL) is the transportation of heavy objects such as waste storage casks or barrels from one location to another through cluttered process facility environments or storage facilities. Typically, an object is lifted by a crane hook on the end of a cable, creating a pendulum that is free to swing during transit. This swinging motion makes remote positioning of casks or barrels difficult to control precisely and is potentially destructive to facility equipment and to other storage containers. Typically, a crane operator moves objects slowly to minimize induced swinging and allow time for oscillations to dampen, maintaining safety but greatly decreasing the efficiency of operations. Using damped-oscillation control algorithms is one approach to solving this problem. This paper summarizes recent simulation results in damped-oscillation-type control algorithms. It also discusses practical implementation issues including control algorithm robustness to payload length changes, hardware requirements for implementation of the control algorithms, and system limits on Coulomb friction.

1.0 INTRODUCTION AND BACKGROUND

Damped-oscillation control algorithms have been demonstrated over the past several years on laboratory-scale robotic systems, on medium-scale gantry robots, and on full-scale overhead cranes. Damped-oscillation crane control was first implemented on a laboratory-scale test at the Sandia National Laboratories using a CIMCORP XR 6100 gantry robot, a 50-lb weight, and an 80-in. cable.[1] This class of algorithms was further analyzed in Singer and Seering,[2,3] Singhose and Singer,[4] Petterson et al.,[5] and Singhose et al.[6] ORNL implemented a damped-oscillation algorithm on a full-scale crane.[7] Work on these types of control algorithms is still an active area of research today (see for example[8,9]). Some of the past implementations of damped-oscillation control on crane-like systems had two shortcomings: (1) they relied on knowledge of the pendulum characteristics of the suspended payload (model-based control), and (2) they were unable to accept moves that were not completely known in advance. The first shortcoming means that the length of the pendulum must be known prior to motion; however, in real operations, the payload center of gravity and total pendulum length would be difficult to determine a priori, especially within hot cell constraints. The second shortcoming is also detrimental to real operations since an operator with either remote video viewing or direct line-of-sight viewing runs typical industrial cranes. For any practical application, provisions must be made for unknown cable lengths and operator-in-the-loop motion. Both the early Sandia and ORNL systems were computerized dc motor-driven systems and not typical examples of industrial facility cranes. Most industrial cranes (>95%) and, in particular older DOE hot cell facility cranes, are driven by ac induction motors. Induction motors are inherently more reliable, more likely to be maintenance free, and capable of being designed to be more radiation tolerant than dc motors; therefore, there is considerable incentive to continue to make new facility cranes ac-motor driven. Also, retrofitting existing ac driven facility cranes with new ac drive technology could help minimize remote construction and rewiring operations for facility conversion. Greatly improved commercial variable-speed ac drives (called flux vector drives) are now on the market. These flux vector inverter drives allow the ac induction motor to be controlled over a wide speed range similar to dc servopositioning systems. The applicability of flux vector drive hardware to this control application was demonstrated for 1-degree-of-freedom on an actual industrial crane in Noakes et al.[10] The remainder of the paper is organized as follows: a section on the analytical development of a model, a section on analytical results, a discussion of some simple experiments, and conclusions.

2.0 ANALYTICAL DEVELOPMENT

In this section an analytical model for a prototypical crane system is derived. A simple model for a crane and its suspended payload system is to consider the system as a rigid-body pendulum, shown in Figure 1 on the following page. Table 1, on the page following Figure 1, defines the symbols used in Figure 1 and in the ensuing analytical development.

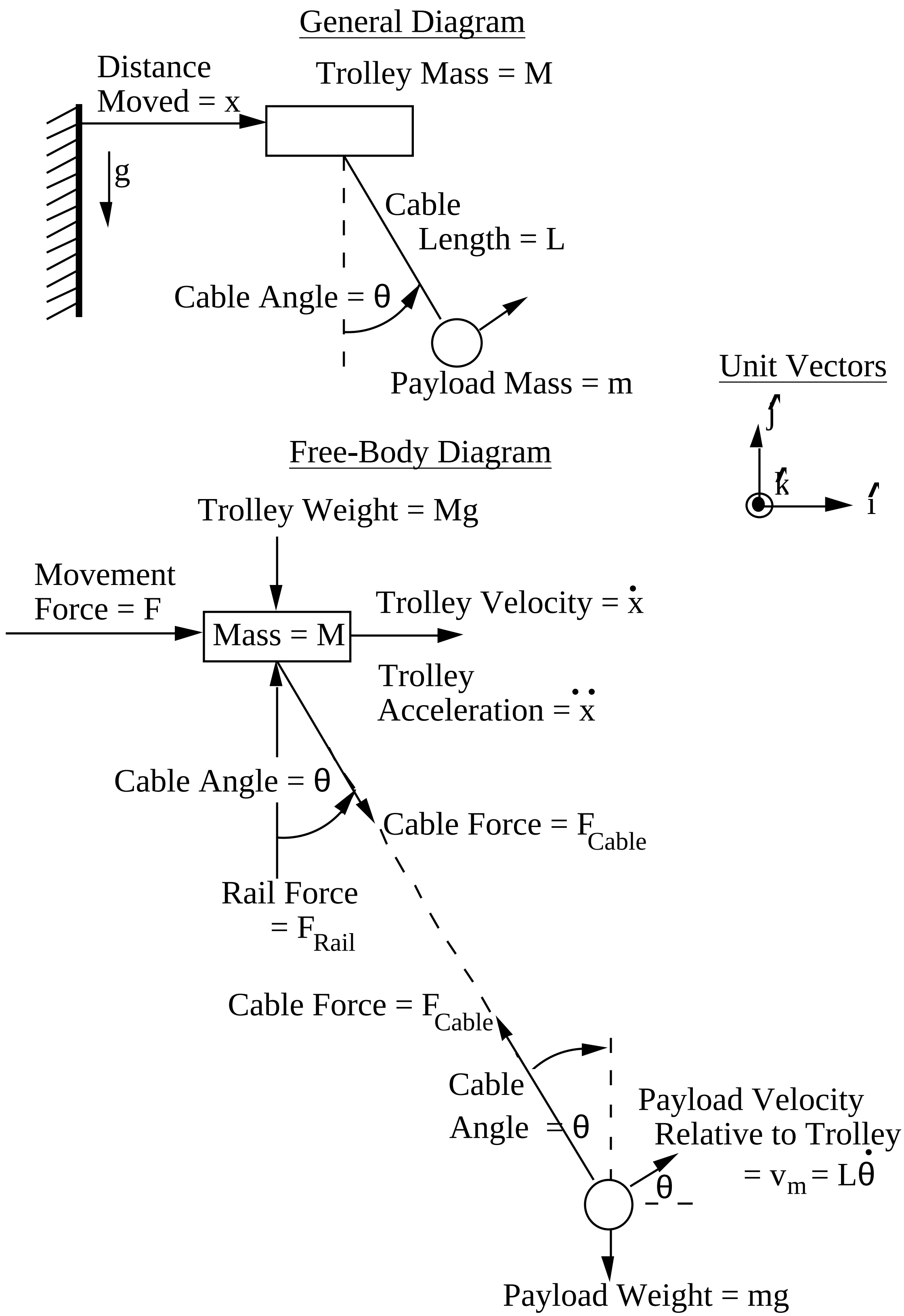

Figure 1. A simple model of a crane trolley and its suspended payload.

Table 1. Symbols used in Figure 1 and in the analytical development.

Symbol	Definition
a	Acceleration (m/s)
F	Force (N)
g	Acceleration due to gravity (10 m/s^2)
L	Cable length (m)
M, m	Trolley and payload mass, respectively (kg)
v	Velocity (m/s)
x	Trolley position (m)
θ	Cable angle (rad)
i, j, k	Unit vectors (-)

Assuming that the cable and crane are not flexible, that the center of gravity of the payload is located at L, that there is no damping or other dissipative forces, and that there is motion in only one plane, then the equation governing the physical behavior of the pendulum system can be easily derived. Note that all of the symbols used in this development were defined in Table 1. Consider applying Newton's second law in the x direction (ΣF_x = mass X a_x) and y direction (ΣF_y = mass X a_y) to the trolley, which gives one the following equations:

$$F + F_{Cable}\sin\theta = M\ddot{x} \quad \text{, and} \tag{1}$$

$$Mg + F_{Cable}\cos\theta = F_{Rail} \quad . \tag{2}$$

Now consider applying Newton's second law to the payload. The velocity of the payload is described by the following equation:

$$\bar{v} = \dot{x}\hat{i} + L\dot{\theta}\cos\theta\,\hat{i} + L\dot{\theta}\sin\theta\,\hat{j} \quad . \tag{3}$$

Taking the derivative of the velocity defined in equation (3) with respect to time provides the payload acceleration in equation (4):

$$\bar{a} = \ddot{x}\hat{i} + L\ddot{\theta}\cos\theta\,\hat{i} - L\dot{\theta}^2\sin\theta\,\hat{i} + +L\ddot{\theta}\sin\theta\,\hat{j} + L\dot{\theta}^2\cos\theta\,\hat{j} \quad . \tag{4}$$

Take the x and y components of the acceleration from equation (4) and use Newton's second law to obtain:

$$-F_{Cable}\sin\theta = m\left(\ddot{x} + \ddot{\theta}L\cos\theta - \dot{\theta}^2 L\sin\theta\right) \text{, and} \tag{5}$$

$$F_{Cable}\cos\theta - mg = m\left(\ddot{\theta}L\sin\theta + \dot{\theta}^2 L\cos\theta\right) \quad . \tag{6}$$

Make the assumptions that θ and $d\theta/dt$ are small, thus

i) Small θ implies that $\cos\theta \approx 1$ and $\sin\theta \approx \theta$,

ii) $d\theta/dt$ small implies that $(d\theta/dt)^2 \approx 0$.

Using assumptions (i) and (ii) above, equations (1), (2), (5) and (6) now become respectively:

$$F + F_{Cable}\theta = M\ddot{x} \quad , \tag{7}$$

$$Mg + F_{Cable} = F_{Rail} \quad , \tag{8}$$

$$-F_{Cable}\theta = m\left(\ddot{x} + \ddot{\theta}\, L\right) , \tag{9}$$

$$F_{Cable} = m\left(g + \ddot{\theta}\, \theta\right) . \tag{10}$$

Substitute equation (9) into equation (7) to obtain:

$$F = \left(M + m\right)\ddot{x} + mL\ddot{\theta} \quad . \tag{11}$$

Substitute equation (10) into equation (9) and note that small θ implies that $\theta^2 \approx 0$:

$$-\ddot{x} = \ddot{\theta}\, L + g\theta \quad . \tag{12}$$

Combine equations (11) and (12) to obtain:

$$F = -ML\ddot{\theta} - \left(M + m\right)g\theta \quad , \tag{13}$$

or restating equation (13) in a LaPlace transform form:

$$F = -\left[MLs^2 + \left(M + m\right)g\right]\theta \quad . \tag{14}$$

Rearrange equation (14) to obtain:

$$\frac{\theta}{F} = \frac{-1}{MLs^2 + \left(M + m\right)g} \quad . \tag{15}$$

Multiply equation (15) by Mg and define $\omega_{ni}^2 = g/L$ to obtain:

$$\frac{\theta}{F/Mg} = \frac{-1}{s^2/\omega_{ni}^2 + \left(1 + m/M\right)} \quad . \tag{16}$$

The transfer function model of equation (16) will be used in two of the studies in the analytical results section that follows.

3.0 ANALYTICAL RESULTS

3.1 Introduction

The model derived in the previous section is assumed to represent the simple physics of a crane with a suspended payload. It was further assumed that position commands to the simple crane model would be prefiltered with an open-loop controller so that command inputs would have a reduced affect on naturally induced vibrations. With these assumptions, an analysis was undertaken to examine three very specific implementation issues with respect to applying the prefiltering control technique to <u>real</u> crane systems. These issues were the following.

1) How many increments of speed are required to have effective control? (That is, what is the required **speed discretization** of the ac motor controller?)
2) What is the effect of having the prefilter tuned to a frequency different from the crane system's natural frequency? (That is, how robust is the controlled system with respect to the tuning of the controller prefilter to the actual length of the payload's cable. This will be studied by modifying the modeled crane system's payload cable length by a **length factor**.)
3) How does stiction and Coulomb friction affect the damped oscillation control? (That is, what is the contribution of stiction and Coulomb friction to the residual vibration?)

The controller prefilter used for the analytical studies is a simple notch filter. The transfer function formulation for a notch filter is given by:

$$\frac{V_{Out}}{V_{In}} = \frac{s^2/\omega_n^2 + 1}{s^2/\omega_n^2 + 2\zeta/\omega_n\, s + 1} \quad , \tag{17}$$

where ω_n is the desired filter frequency (usually the natural frequency of the system being controlled) and ζ is the damping ratio. It is desired to design a notch filter as an open-loop filter for the crane system with a natural frequency of 1 rad/s (2π Hz) and a damping ratio of 0.5. For $\omega_n = 1$ and $\zeta = 0.5$, the notch filter transfer function is:

$$\frac{V_{Out}}{V_{In}} = \frac{s^2 + 1}{s^2 + s + 1} \quad . \tag{18}$$

The first two studies (discretization and tuning) utilize a normalized transfer function model for the analysis. For this case, the system transfer function from equation (16) is rearranged to give:

$$\frac{\theta}{F/ML\omega_n^2} = \frac{-1}{s^2/\omega_n^2 + 1} \quad , \tag{19}$$

where

$$\omega_n^2 = \frac{g}{L}\left(1 + \frac{m}{M}\right) \quad . \tag{20}$$

The stiction/Coulomb friction study does not use the transfer function representation of equation (16). Instead, it uses a physical model based on equation (13) with the driving force reduced by a nonlinear friction force. (Recall also that stiction and Coulomb friction are nonlinearities and transfer function representations are reserved for linear systems only.)

3.2 Results for Residual Vibration versus Speed Discretization. [Uses the normalized transfer function model of equation (19).]

The goal of this study is to determine how many speeds are required for effective control. The approach is to examine residual vibration that is defined as the ratio of the vibration remaining in the crane payload system at steady state following a step input. The parameters used for this study are:

1) Natural frequency = ω_n = 1 rad/s (A reasonable natural frequency for small payload and large trolley mass), and
2) Normalized step input =$F/ML\omega_n^2$ = 1.

The independent variable is speed discretization which is defined as the number of steps in the actuator output; i.e., 10:1 means one has 0, 0.1*(full scale), 0.2*(full scale),..., (full scale) available for control. Figure 2 shows normalized residual vibration ($\theta/F/ML\omega_n^2$) versus speed discretization. The effect of a mismatch of the control prefilter to the crane system natural frequency on the speed discretization results is also examined. The curves with different percentages shown in Figure 2, on the following page, are the amount that the actual system natural frequency varies from the prefilter frequency. For example, the -1% shown in Figure 2 is a case where the system transfer function is $1/[s^2/(1\text{-}0.01)^2 + 1]$. The conclusion from this analysis is to use motor and motor control hardware having a speed discretization capability >= 10:1 because speed discretizations less than 10 showed greatly increased residual vibration.

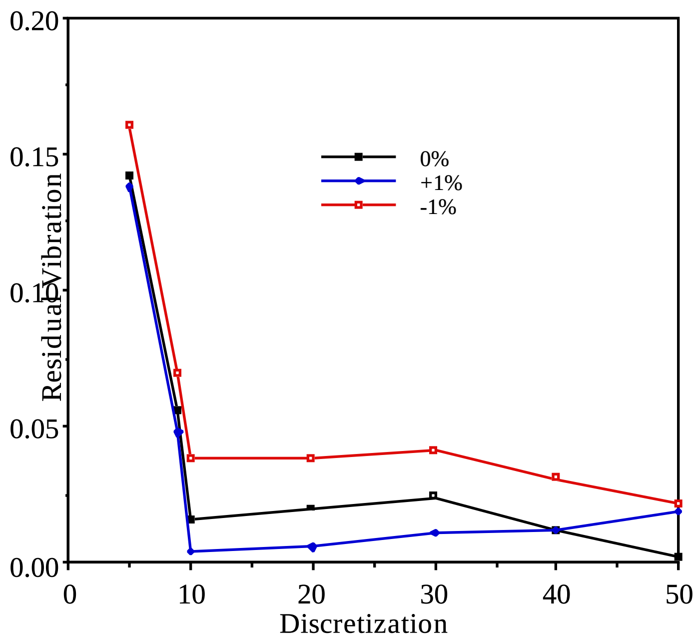

Figure 2. Normalized residual vibration (_/F/ML_$_n^2$) versus speed discretization for different control prefilter tunings.

3.3 Results for Residual Vibration versus Length Factor. [Uses the normalized transfer function model of equation (19).]

The goal of this study is to determine how prefilter and system mismatch affect control. The approach is to examine residual vibration for different levels of prefilter/system mismatch. The parameters used for this study are:

1) Natural frequency = ω_n = 1 rad/s (A reasonable natural frequency for small payload and large trolley mass), and
2) Normalized step input $=F/ML\omega_n^2 = 1$.

The independent variable is Length Factor (LF) defined by the following. The crane system's new length = LF*(The original crane system length), where LF is the "Length Factor." Thus, an LF of 1 implies that the crane system model has a length that is unchanged, an LF of 3.5 means the length is 3.5 times longer than the original crane system length (that is, the length that the prefilter was tuned to), etc. Speed discretization is set to a very high number so that it has no effect. The results are shown in Figure 3.

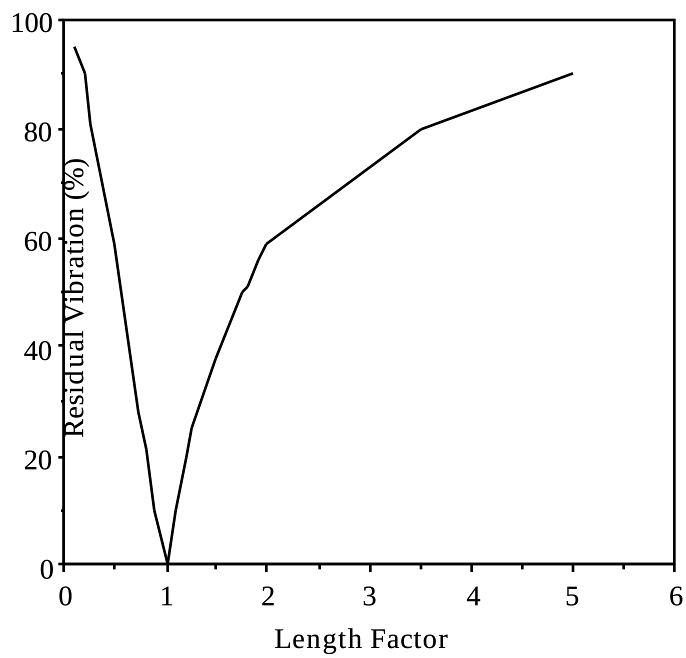

Figure 3. Normalized residual vibration ($\theta/F/ML\omega_n^2$) versus length factor for a filter tuned to a system having a natural frequency of 1 rad/s and a normalized step input of 1.

Other natural frequencies showed similar trends. The conclusions from this analysis are the following.
1) To avoid significant residual vibration, operate the crane to within 0.8 to 1.2 of the prefilter tuned length.
2) A higher order prefilter or a different control approach might be necessary for applications that have significant variation in crane system length.

3.4 Results for Stiction/Coulomb Friction Analysis. (Uses a physical model.)

The goal of this study is to determine the effects of stiction and Coulomb friction on residual vibration. The approach is to examine residual vibration for different levels of friction. In this case, a physical model was used based on equation (13) and a velocity step input was used as the control input to the prefilter. The parameters used for this study are:

1) Velocity step input = 1 m/s,
2) Trolley mass: M=1000 kg,
3) Payload mass: m=10 kg,
4) Payload cable length: L = 10 m,

The filter is tuned exactly to the system natural frequency, that is, there is no filter error in this case. The system and controller were modeled using MATLAB. The results of the study are presented in Table 2. Note: for these parameters and the 1 m/s input, the steady-state angle of the crane system is approximately 0.1 rad.

Table 2. Results from the stiction/Coulomb friction study.

Stiction/Coulomb Friction Ratio	Stiction Friction (N)	Coulomb Friction (N)	Residual Vibration (rads)
2/1	50	25	0.005
2/1	100	50	0.010
2/1	200	100	0.020
2/1	300	150	0.031
2/1	400	200	0.042
1.5/1	37.5	25	0.006
1.5/1	50	33.3	0.007
1.5/1	75	50	0.010
1.5/1	100	66.6	0.013
1.5/1	150	100	0.020
1.5/1	200	133.3	0.024
1.5/1	225	150	0.030
1.5/1	300	200	0.040
1.5/1	400	266.6	0.054
1/1	25	25	0.005
1/1	50	50	0.010
1/1	100	100	0.020
1/1	150	150	0.030
1/1	200	200	0.040
1/1	300	300	0.060
1/1	400	400	0.080

The conclusions from this portion of the analysis are the following.
1) Stiction has little effect on residual vibration.
2) Residual vibration is linearly proportional to Coulomb friction.

4.0 PAST EXPERIMENTAL RESULTS SUPPORTING SIMULATIONS

Experimental results were previously reported.[11] The experimental hardware is located in the Robotics & Process Systems Division (RPSD) of Oak Ridge National Laboratory (ORNL). The hardware is an ac-motor driven crane that has been retrofit with updated flux vector inverter drives and motor packages for both the bridge and trolley drives. A VME-based computer control system has also been added. The RPSD crane is a 30-year-old CONCO 25-ton-capacity/3-ton auxiliary crane with all ac motor control. The original ac bridge motor is a 5-hp unit controlled by a switch box. The original trolley motor is 3 hp. Thor, Inc., makes the new motor drive hardware. The new motors are three-phase, 480-V ac motors. 7.5-hp bridge and a 5.0-hp trolley motors were used. The flux vector drive has almost 1000:1 speed range capability. All of the motor control hardware is mounted on the crane trolley, and the computer system is mounted on the bridge. (The computer was mounted on the bridge because there was insufficient space on the trolley.) A festooning device is used to distribute control signals from the bridge to the trolley-mounted hardware. A tethered pendant is used for the control interface. The crane's original radio-frequency pendant remains operable as a safety switch for the test system.

A version of the prefilter controller was implemented on this system and was tested using a suspended payload having a natural frequency of 0.135 Hz. The demonstration used a ~14-m-long pendulum and moves of several meters in two simultaneous directions. Top speeds of ~1m/s were obtained. Comparing typical runs with and without the damped-oscillation controller showed residual vibrations being reduced from ±30 cm to ±3 cm (an order of magnitude reduction). Note that this vibration is equivalent to $\sim 2 \times 10^{-3}$ rads. Experiments to determine the speed reduction range necessary for good swing-free control supported the conclusion that 10:1 variability is sufficient. The present implementation of the control algorithm can reduce oscillations over large changes in pendulum length. In a typical experiment, the cable length was changed by a factor of four and the residual vibration increased from ±3 cm to ±7 cm (over 200%). The changes in pendulum length can occur while the other degrees of freedom are moving.

5.0 CONCLUSIONS

This paper describes a simple model of a crane/payload system. This model was used to make several conclusions concerning implementation of simple prefiltering techniques as a way of damping oscillations in crane motion. The analysis determined the following.

1) Motor control hardware needs speed discretizations >= 10:1.
2) To avoid significant residual vibration, operate the crane to within 0.8 to 1.2 of the prefilter tuned length.
3) A higher order prefilter or a different control approach might be necessary for applications that have significant variation in crane system length.
4) Stiction has little effect on residual vibration.
5) Residual vibration is linearly proportional to Coulomb friction.

Future efforts will focus on further experimental verification of these results and also might focus on one or more of the following: 1) Coupled drives, 2) Moving base, 3) Polar cranes.

REFERENCES

1. Jones, J. F., and Peterson, B. J., "Oscillation Damped Movement of Suspended Objects," pp. 956–962, in *Proceedings of 1988 IEEE International Conference on Robotics and Automation, Philadelphia, PA, April 24-29, 1988.*
2. Singer, N. C., and Seering, W. P., "Design and Comparison of Command Shaping Methods for Controlling Residual Vibration," pp. 888–893, in *Proceedings of 1989 IEEE International Conference on Robotics and Automation, Scottsdale, AZ, May 14-19, 1989.*
3. Peterson, B. J., Robinett, R. D., and Werner, J. C., "Parameter-Scheduled Trajectory Planning for Suppression of Coupled Horizontal and Vertical Vibrations in a Flexible Rod," pp. 916–921, in *Proceedings of 1990 IEEE International Conference on Robotics and Automation, Cincinnati, OH, May 13-18, 1990.*
4. N. C. Singer and W. P. Seering, "Preshaping Command Inputs to Reduce System Vibration," ASME J. Dyn. Sys. Meas. and Control, Vol 112, pp. 76-82, March 1990.
5. W. E. Singhose and N. C. Singer, "Effects of Input Shaping on Two-Dimensional Trajectory Following," IEEE Trans. on Robotics and Automation, Vol. 12, No. 6, pp. 881-887, Dec. 1996.
6. Singhose, W. E., Seering, W. P., and Singer, N. C., "Shaping Inputs to Reduce Vibration: A Vector Diagram Approach," pp. 922–927, in *Proceedings of 1990 IEEE International Conference on Robotics and Automation, Cincinnati, OH, May 13-18, 1990.*
7. Noakes, M. W., Petterson, B. J., and Werner, J. C., "An Application of Oscillation Damped Motion for Suspended Payloads to the Advanced Integrated Maintenance System," *American Nuclear Society Annual Meeting, June 10-14, 1990*.
8. Singhose, W., Singh, T., and Seering, W., "On-Off Control with Specified Fuel Usage," *J. Dyn. Sys. Meas. And Control*, **121**, pp. 206-212, June 1999.
9. Lim, S. Stevens, H. D., and How, J. P., "Input Shaping Design for Multi-Input Flexible Systems," *J. Dyn. Sys. Meas. And Control*, **121**, pp. 443-447, Sept. 1999.
10. Noakes, M. W., Kress, R. L., and Appleton, G. T., "Implementation of Damped-Oscillation Crane Control for Existing ac Induction Motor-Driven Cranes," *American Nuclear Society Annual Meeting, April 25-30, 1993,* pp. 479–485.
11. Kress, R. L., Jansen, J. F. and Noakes, M. W., "Experimental Implementation of a Robust Damped-Oscillation Control Algorithm on a Full-Sized, Two-Degree-Of-Freedom, AC Induction Motor-Driven Crane," in the *Proceedings of the Fifth International Symposium on Robotics and Manufacturing*, Vol. 5, Maui, HI., Aug. 14-18, 1994.